AECL-8366

ATOMIC ENERGY OF CANADA LIMITED

L'ENERGIE ATOMIQUE DU CANADA, LIMITEE

THE EFFECT OF pH ON THE STABILITY OF SMECTITE

L'EFFET DU pH SUR LA STABILITE DE LA SMECTITE

R. M. Johnston, H. G. Miller

Whiteshell Nuclear Research Establishment

Etablissement de recherches nucléaires de Whiteshell

Pinawa, Manitoba R0E 1L0

November 1984 novembre

ATOMIC ENERGY OF CANADA LIMITED

THE EFFECT OF pH ON THE STABILITY OF SMECTITE

by

R.M. Johnston and H.G. Miller

Whiteshell Nuclear Research Establishment
Pinawa, Manitoba ROE 1LO
1984 November

AECL-8366

L'EFFET DU pH SUR LA STABILITÉ DE LA SMECTITE

par

R.M. Johnston et H.G. Miller

RÉSUMÉ

On a étudié expérimentalement la stabilité hydrothermique de la smectite à des températures inférieures à 275°C pour une série de valeurs de pH. Dans la partie à pH presque neutre, la conversion smectite-illite a prédominé; dans la partie légèrement acide, il y avait une formation importante de couches intercalées d'hydroxyaluminium dans l'argile; dans la partie alcaline, des silicates de structure (feldspath et zéolites) ont été produites. On étudie l'évidence géologique de ces réactions.

L'Énergie Atomique du Canada, Limitée
Établissement de recherches nucléaires de Whiteshell
Pinawa, Manitoba ROE 1LO
1984 novembre

AECL-8366

THE EFFECT OF pH ON THE STABILITY OF SMECTITE

by

R.M. Johnston and H.G. Miller

ABSTRACT

The hydrothermal stability of smectite at temperatures less than 275°C was investigated experimentally over a range of pH values. In the near-neutral pH region, the smectite to illite conversion predominated; in the mildly acid region, there was extensive formation of aluminum hydroxy interlayers in the clay; and in the alkaline region, framework silicates (feldspar and zeolites) were produced. The geological evidence for these reactions is also reviewed.

Atomic Energy of Canada Limited
Whiteshell Nuclear Research Establishment
Pinawa, Manitoba ROE 1LO
1984 November

AECL-8366

CONTENTS

1. INTRODUCTION

Bentonite has suitable physical and chemical properties for use as a component of the buffer and backfill for the deep underground disposal of nuclear fuel wastes in the Canadian Nuclear Fuel Waste Management Program [1,2]. Elevated temperatures (from 100 to 150°C) and the presence of groundwater in the disposal vault raise the possibility of the hydrothermal alteration of the bentonite.

The hydrothermal stability of smectite has been studied extensively. Much of the work has centred on the collapse of expandable smectites to non-expandable layer silicates, in particular the formation of illite. Eberl and his co-workers [3,4,5] have defined a series of reaction trends from smectite to non-expandable phyllosilicates (illite, micas, chlorites) by way of mixed-layer clay minerals, with the precise reaction trend being determined largely by the interlayer cations. However, in a number of studies, the formation of framework silicates as well as, or instead of, clay minerals has been reported. This is particularly true of studies conducted in alkaline systems. Inoue [6] reports formation of the calcium zeolites, wairakite and heulandite, as well as illite and smectite, from the reaction of calcium montmorillonite with 0.2 mol/L KOH at 300°C. Komarneni and White [7] have reported the formation of strontium feldspar, strontium wairakite and strontium åkermanite from the interaction of $Sr(OH)_2$ solutions with a variety of clays and shales at 200°C and 300°C. In an earlier study [8], pollucite (an anhydrous cesium analogue of wairakite) and $CsAlSiO_4$ (a cesium analogue of nepheline) were produced in the same clays using CsOH at 100, 200 and 300°C. Feldspar was commonly observed amongst the reaction products in hydrothermal tests on sodium and potassium montmorillonite between 260 and 400°C by Eberl and his co-workers [3,4].

The aim of our study was to assess the significance of low-temperature smectite transformations yielding products other than clay minerals, and the dependence of smectite stability and reaction trends on

pH. An experimental study of smectite stability was conducted under a range of pH conditions, at temperatures between 150 and 275°C. These temperatures are somewhat higher than the 25 to 150°C expected in a nuclear waste disposal vault, but the kinetics of clay reactions are very slow, even at 275°C. The geological evidence for smectite transformations in alkaline systems and the formation of aluminum hydroxy interlayers in acidic systems is also reviewed.

2. EXPERIMENTAL PROCEDURE

Sodium and calcium montmorillonite were reacted with potassium-bearing solutions over a range of pH values, at 150, 200 and 275°C. K^+ was chosen as the dominant solution cation, since it has been shown to promote the conversion of smectite to illite [3,9]. Earlier studies had shown that montmorillonite, slurried with distilled deionized water or salt solutions, undergoes a rapid decrease in pH from mildly alkaline (pH = 8 to 9) to mildly acidic (pH ≈ 3 to 6) when treated at temperatures of 150 to 275°C (Johnston and Miller, unpublished results). Therefore, varying amounts of bicarbonate or hydroxide were added to buffer the pH in the required region.

2.1 STARTING MATERIAL

The clay fraction (< 2 μm) of a calcium bentonite (Pembina Mountain Filtaclay 75 [10]) was used as the starting material in all experiments. The clay material was prepared using the methods described by Miller [11]. Cation exchange positions were saturated with either Na^+ or Ca^{2+} (using the appropriate chloride) to yield a homoionic clay. The clay fraction was characterized using X-ray diffraction (see Section 2.4) and was found to be almost pure montmorillonite, with a trace of quartz. A small 1.4-nm* component that does not expand on saturation with glycerol

---

* 1nm = 10 Å.

was attributed to the presence of aluminum hydroxy interlayers in the montmorillonite (see Section 4.2). The Greene-Kelley test [12] yielded no indication of the presence of beidellite (see Figure 1).

2.2 RUN 1

For the first run, small, stainless-steel, Parr pressure vessels with Teflon liners were used. The clay was mixed with KCl solutions varying in concentration from 0.01 to 1.0 mol/L (see Table 1). The clay to solution ratio was 1:50 by weight (200 mg in 10 g). In four of the samples, a mixed bicarbonate-chloride solution, with $HCO_3^-/Cl^- = 3/2$, was used to buffer the pH in the mildly alkaline range. The pH of the slurry was measured at 25°C before and after heating, using a Cole Parmer Chemcadet pH meter. The samples were held at 275°C for 30 days. Water loss from the Teflon liners was evident in most samples, and was considerable in some, so final pH values are only approximate.

2.3 RUNS 2, 3 and 4

In Runs 2,3 and 4, the clay was mixed with KCl/KOH solutions with the K^+ concentration constant at 0.1 mol/L, and the OH^- concentration variable, as shown in Tables 2, 3 and 4. The runs were carried out in sealed gold tubes in an autoclave - Run 2 at 275°C for 15 days, Run 3 at 200°C for 27 days, and Run 4 at 150°C for 30 days.

Gold tubing with an outside diameter of 0.8 cm and a wall thickness of 0.013 cm was annealed at 700°C for 3 h, and cut into 10-cm sections that were sealed at one end by a cold-welding device. Then, 50 mg of clay and 2.5 mL of solution were added, and the clay was dispersed using an ultrasonic probe. The initial pH was measured using a Cole Parmer Chemcadet pH meter with a Fisher pencil-thin combination pH electrode. The tube was sealed using a cold-welding device.

The sealed tubes were placed in a special holder to keep them upright in the autoclave. Water was added to the autoclave to balance the

pressure buildup in the gold tube at the temperature of the run. The autoclave was sealed, placed in a heating mantle and brought to the desired temperature. When the run was complete, the gold tubes were cut open at one end and the pH was measured at 25°C.

It should be noted that the pH measurements were made in a slurry, in quite concentrated salt solutions, and so do not have high precision. They were, however, reproducible to within ± 0.5 pH units.

2.4 X-RAY DIFFRACTION ANALYSIS

The products from each run were dispersed in distilled water and an oriented powder mount was prepared for X-ray diffraction (XRD) analysis, as described by Miller [11]. A preliminary XRD scan was performed, and those samples with appreciable amounts of phyllosilicates were washed repeatedly with $MgCl_2$ to give a homoionic magnesium smectite for consistency in XRD analysis, and again prepared as oriented mounts. Samples in which appreciable amounts of phases other than phyllosilicates were detected were prepared as randomly oriented powder mounts.

X-ray diffraction analysis was carried out using a Philips diffractometer with a graphite crystal monochromater and cobalt Kα radiation. Normal running conditions were 45 kV and 30 mA. Samples were prepared using a rutile internal standard with a strong peak at 0.323 nm. Cobalt Kα radiation was used since its relatively long wavelength (0.1790 nm) gives good resolution for the low-angle diffraction peaks.

It is difficult to quantify mineral proportions from XRD data, especially from oriented samples. It cannot always be assumed that the phase with the strongest peaks is the most abundant, since peak intensity also depends on the degree of crystallinity. In clay samples, most minerals have a lower detection limit by XRD of 5 to 10%.

2.5 IDENTIFICATION OF CLAY MINERALS

Clay minerals were identified on the basis of their basal spacings at 52% relative humidity (RH) over saturated $Mg(NO_3)_2$ solution, and solvated with glycerol. The homoionic Mg^{2+} form of the expandable clays was used, to provide consistency. Typical basal spacings for various magnesium smectites are given in Table 5 [13], and it can be seen that vermiculite (with a negative layer charge $\geq 0.5/O_{10}$) can be distinguished from lower charge smectites using this method. Beidellite (with a net negative charge in tetrahedral positions) can be distinguished from montmorillonite (with a net negative charge in octahedral positions) using glycerol solvation of the lithium-saturated form after heating to 300°C (Greene-Kelley test) [12].

The literature on determination of the extent of interlayering of smectite with 1-nm illitic phases is extensive and complex [14,15,16]. The most common method uses shifts in the (001) peaks, from 1.5 nm (for magnesium smectite at RH = 54%) towards 1 nm. Ordered interlayering can result in a peak at 1 + 1.5 = 2.5 nm (2.8 nm with glycerol). Irrational higher order peaks are indicative of random interlayering, as there is a tendency for adjacent peaks to coalesce and give a peak with intermediate spacing. For instance, d_{003} (1.0 nm) at 0.33 nm and d_{005} (1.5 nm) at 0.30 nm may give a combined broad peak in the region of 0.32 nm. In this study, such peak shifts have been used to identify the presence of interlayered illite-smectite, but no attempt has been made to quantify the extent of interstratification, except in very general terms.

A complicating factor is introduced by the possibility of forming aluminum hydroxy interlayers in the smectite that fix the basal spacing at about 1.4 nm and prevent further swelling (see Section 4.2). A highly charged magnesium smectite or vermiculite gives a very similar XRD pattern, since it has d_{001} = 1.43 nm, both with glycerol and at 54% RH. The two can be distinguished only by removal of the aluminum hydroxy interlayer, after which a smectite with low layer charge will re-expand to 1.8 nm with

glycerol solvation. Treatment with 1 mol/L sodium tartrate for 24 hours at 60°C effectively removes the aluminum hydroxy interlayer [17].

3. RESULTS

3.1 RUN 1

The results from Run 1 are given in Table 1. Final pH values fell into two distinct groups: pH 3 to 4 for samples in which the pH was allowed to vary freely; pH 8 to 10 for those in which the pH was buffered by bicarbonate. The sodium smectite produced consistently lower pH values for the first procedure and higher values for the second procedure than calcium smectite.

The pH had a dramatic effect on the reaction products. All samples run at the high pH produced the same results, regardless of K^+ concentration and calcium or sodium saturation. Figure 2 shows a typical XRD trace. The following phases were identified:

- analcime-type zeolite
- potassium feldspar (high sanidine)
- boehmite and diaspore (γ- and α-AlOOH)
- quartz
- ferrihydrite (hydrous iron oxides)
- some poorly crystalline illite/smectite.

As shown in Table 6, the feldspar peaks observed match those of high sanidine (X-Ray Powder Diffraction File (XRPDF) 10-353) [18], a disordered phase commonly formed in short-term hydrothermal runs. The remaining peaks correspond overall to those of a zeolite with the analcime structure (XRPDF 7-363) [19]. Analcime ($NaAlSi_2O_6 \cdot H_2O$) and its calcium analogue, wairakite, are the most common zeolites with this structure, but analogous structures can be formed with a variety of cations. Potassium,

cesium and rubidium forms are usually anhydrous and are classified as feldspathoids. However, hydrous potassium analcime can be formed, and substitution of potassium and calcium into the analcime framework is quite common. The larger size of the K^+ ion distorts the lattice somewhat, which may account for the slight departure from the given spacings. The formation of an analcime-type zeolite is in general agreement with the stability field defined by Barrer [20] for zeolites forming from aqueous $Na_2O{\cdot}Al_2O_3{\cdot}nSiO_2$ hydrogels (see Figure 3).

The clay phase in these samples gives a broad peak between 1 and 1.2 nm, indicating a phase that is dominantly illitic, with a small expandable component.

A completely different reaction was observed when the pH was allowed to vary freely and finally decreased to 3 to 4. Illite and mixed-layer illite/smectite were formed, and considerable variation in the extent of the reaction was observed, depending on the K^+ concentration and whether Na^+ or Ca^{2+} was present as the interlayer cation. For the calcium smectite, no reaction was observed for K^+ concentrations less than 0.01 mol/L, except for the disappearance of the 1.4-nm peak in the glycerol-solvated samples, which is attributed to dissolution of aluminum hydroxy interlayers. It is important to note that a K^+ concentration of 0.02 mol/L was required to provide sufficient K^+ to saturate the exchange positions of the clay and that no reaction was observed until the K^+ concentration was considerably above this level. As the K^+ concentration was increased from 0.05 to 1 mol/L, the 1.0-nm peak increased and the (001) smectite peak broadened out towards 2.8 nm and 1.4 nm, indicating the buildup of mixed-layer clays.

For the sodium smectite, no reaction was observed at $[K^+] = 0.01$ mol/L, but the reaction products for $[K^+] = 0.1$ mol/L were identical to those for $[K^+] = 0.5$ mol/L with calcium smectite. With $[K^+] = 0.5$ mol/L, sodium smectite converted to an ordered mixed-layer illite-smectite (rectorite) with a distinct, strong 2.8-nm peak. Figure 4 illustrates these reaction trends.

Samples 1.4 and 1.12 were tested for beidellite using the Greene-Kelley test. In both cases the (001) peak was broadened to about 1.2 nm, a considerable shift from the 0.95-nm peak of the starting material. This indicates that some charge buildup occurred in the tetrahedral layer, as predicted by Eberl et al. [21], as a precursor to the collapse to illite.

In summary, the K^+ concentration had a very strong effect on the extent of the transformation from smectite to illite, with no reaction observed when the K^+ concentration was less than that of the interlayer cation. The transformation of sodium smectite proceeded much more quickly than that of calcium smectite, in keeping with the results of Eberl [3] and Roberson and Lahann [9].

3.2 RUN 2

In Run 2, after 15 days at 275°C, the final pH of the samples ranged from 3 to 12 (see Table 2). As in Run 1, the final pH was more acidic for the sodium smectite than for the calcium smectite. Because of the buffering capacity of the clay, the pH changed rapidly with small additions of OH^- in the neutral region. At OH^- concentrations less than 0.025 mol/L, the presence of KOH had little effect, and the final pH values were not substantially different from those observed in the pure chloride systems in Run 1.

In samples with the final pH greater than 7, little of the starting smectite remained. Potassium feldspar (high sanidine), quartz and a clay phase, which was dominantly illite, were produced. A fourth phase, present in samples 2.1, 2.9 and 2.10 (all with final pH ≈ 12), has been identified as a phillipsite-type zeolite (XRPDF 12-195) [22] (see Table 7 and Figure 5).

Although there is some discrepancy between observed d-spacings and those reported in the literature, the general pattern of strong peaks matches well, and the differences can be attributed to distortion of the

lattice due to substitutions, or line broadening caused by small crystal size. Phillipsite is a common product in potassium-rich systems in the temperature range 85 to 350°C [20]. An approximate formula is $(K,Na,1/2Ca)_3Al_3Si_5O_{16}\cdot 6H_2O$, but it can accommodate a range of aluminum:silicon ratios and a variety of cations.

In the most alkaline samples, the clay phase was mainly illite (1.0 nm). However, with decreasing final pH, a larger smectite component remained, as indicated by a broad peak at about 1.2 nm, as well as a discrete 1.0-nm peak. There was little change with glycerol solvation, and higher order peaks were broad and close to those of illite (d_{002} ≈ 0.495 nm, d_{003} ≈ 0.33 nm). This suggests that illite was the dominant reaction product and that the proportion of expandable layers was small.

This clay phase was the dominant reaction product for samples in which the final pH was in the acid region, but still above that of hydroxide-free systems (see samples 2.5, 2.6, 2.12, 2.13, and 2.14 in Table 2). Feldspar and quartz were present in small amounts, but no zeolites were detected.

The extent of reaction was much more limited in samples in which the hydroxide had no effect on pH. Small amounts of quartz and illite were detected, but no feldspar. The clay phase was characterized by a broad peak at 1.4 nm, with non-rational higher order peaks (d(002) ≈ 0.48 nm, d(003) ≈ 0.33 nm) that did not expand with glycerol solvation (see Figure 6). However, after treatment with sodium tartrate, the smectite expanded with glycerol solvation to 1.8 nm, producing an XRD pattern virtually indistinguishable from the starting material (Figure 1(b)). Thus, the 1.4-nm spacing in the clay phase was attributed to the formation of aluminum hydroxy interlayers rather than to the presence of a high layer charge or interstratified illite-smectite. The small residual 1.4-nm peak was attributed to incomplete removal of the hydroxy interlayers during treatment with sodium tartrate.

Samples 2.6 and 2.14 were tested for the presence of beidellite and, as in Run 1, a peak shift from 9.5 to 0.10-0.12 nm was observed, indicating the presence of some beidellitic layer charge.

3.3 RUN 3

The reaction products for Run 3, held at 200°C for 27 days, are given in Table 3. Samples with a final solution pH below 6 showed no appreciable reaction beyond formation of a small amount of illite and the development of a 1.4-nm phase due to aluminum hydroxy interlayers. There was no apparent correlation between the amount of 1.4-nm phase and the solution pH. Samples 3.6 and 3.15 were treated with sodium tartrate (as described in Section 2.5), and in both cases the aluminum hydroxy interlayers were almost completely removed by the treatment, indicating that little lattice modification had occurred.

More extensive reaction took place in those samples with a higher pH. Feldspar (high sanidine) was detected in all samples with a final pH greater than 6, and a zeolite identified as phillipsite was found in the most alkaline samples (samples 3.1 and 3.9) (see Figure 7). In these samples, illite was abundant, as well as a mixed-layer illite-smectite characterized by a broad basal peak at 1.0 to 1.2 nm, which showed little change after solvation with glycerol. In samples 3.2, 3.3 and 3.10, the 1.2-nm basal spacing expanded with glycerol solvation to give a very broad peak between 1.0 and 1.8 nm, suggesting a random interstratification of illite and expandable smectite, possibly with a non-expandable 1.4-nm component.

No difference in reaction products for sodium and calcium smectites was observed.

3.4 RUN 4

At 150°C, the only reaction observed after 30 days in any of the samples, regardless of pH, was the production of a small amount of illite

(d = 1.0 nm) in all samples and the development of a 1.4-nm phase (see Table 4). Treatment with sodium tartrate returned the smectite to full expandability, indicating the formation of aluminum hydroxy interlayers rather than true lattice modification. There was no apparent relationship between the solution pH and the extent of production of the 1.4-nm phase. No tectosilicates were detected. Illite peaks were slightly enhanced in the samples with highest final solution pH, particularly in the sodium smectites. No other differences were observed between the reaction of calcium and sodium smectite.

3.5 SUMMARY

(1) Quartz, present in the starting material as a trace constituent, was still present in all reaction products.

(2) A small amount of illite formed even in those samples that showed the least extent of reaction. This was due to the presence of a small number of highly charged layers in the starting smectite, which collapsed irreversibly on contact with K^+ solution.

(3) Aluminum hydroxy interlayers were produced in those samples for which the final pH was mildly acidic, at all three run temperatures.

(4) Zeolites formed at 275°C to give a final pH as low as 8.5 for calcium smectite, and 10 for sodium smectite. At 200°C, zeolites were produced only in the most alkaline samples (pH > 12). Analcime was produced in the bicarbonate systems and phillipsite in the presence of hydroxide.

(5) Feldspar (sanidine) was a very common product at 200 and 275°C, in neutral to alkaline solutions.

(6) Smectite showed little evidence of true lattice modification, even at 275°C, when the pH was allowed to vary freely. In

concentrated KCl solutions (> 0.1 mol/L), some conversion to interlayered illite-smectite occurred, with sodium smectite reacting more readily than calcium smectite.

(7) In alkaline solution, extensive modification of clay structures occurred, with the formation of abundant illite, often with a small, expandable, smectite component. Lattice modification in clays is facilitated by increased aluminosilicate solubility at high pH.

4. DISCUSSION

4.1 pH VARIATION

Smectites are known to buffer pH in aqueous slurries in the mildly alkaline region (pH ∿ 8.5 for calcium smectite, pH ∿ 9 for sodium smectite) due to exchange with the H^+ ion [23]. However, as indicated by samples 2.8, 2.16, 3.8, 3.16, 4.8 and 4.16 in Tables 2, 3 and 4, when treated at temperatures above 100°C, the pH drops rapidly to the acid region (pH = 3 to 6). This effect has also been noted by Eberl [3]. Gerstl and Banin [24] reported a similar, but slower, decrease in pH for calcium smectite held at 30°C for 100 days. The pH reached a steady-state value of 4 within 25 d. The reason for this behaviour is still not completely clear. A similar phenomenon, observed by Bischoff and Seyfried [25] while heating seawater, has been attributed to the precipitation of magnesium oxysulphate and anhydrite.

Although the systems in this study contained very little Mg^{2+} or SO_4^{2-}, it is likely that similar precipitation reactions involving other cations could have occurred. Since most clays contain abundant amorphous material of relatively high solubility and sorptive capacity, the pH is likely controlled by a number of complex reactions. The production of aluminum hydroxy interlayers in the smectite suggests that proton release

during aluminum hydrolysis may be important. The observation that sodium smectite slurries fell to lower pH values than calcium smectites in unbuffered samples may be explained by the greater selectivity of sodium smectite for Al^{3+}, since Al^{3+} replaces monovalent Na^{+} more easily than divalent Ca^{2+}.

Sodium smectite also produced higher final pH values than calcium smectite in systems in which a pH was imposed by an alkaline fluid. Barrer [20] found that, in the synthesis of zeolites, the pH of the fluid after reaction was always highly alkaline for sodium systems but was closer to neutral, or occasionally acidic, for calcium systems.

4.2 ALUMINUM HYDROXY INTERLAYERS

Smectites display a strong preference for trivalent cations over divalent and monovalent cations, so that Al^{3+} is strongly adsorbed. McBride and Bloom [26] found that Al^{3+} was adsorbed by montmorillonite much more strongly than Ca^{2+}, even with abundant Ca^{2+} in solution. This preference was enhanced if aluminum was present as aluminum hydroxy complexes, due to their greater radii and lower hydration energies, allowing stronger electrostatic interaction with the surface. Polymeric aluminum hydroxy ions were also preferred due to entropy effects. Clay surfaces enhance aluminum hydrolysis. Bloom et al. [27] calculated a 2- to 9-fold increase in the degree of hydrolysis of aluminum at clay surfaces compared with that in solution. Adsorption of aluminum is accompanied by hydrolysis and release of H^{+} to solution, resulting in a decrease in pH.

The formation of aluminum hydroxy complexes is favoured in the mildly acid range. At pH < 4, the $Al(H_2O)_6^{3+}$ ion dominates, while gibbsite ($Al(OH)_3$) solubility is at a minimum at pH ≈ 6. Thus, the optimum conditions for the formation of aluminum hydroxy interlayers in clay minerals is at pH ≈ 4 to 6. Aluminum hydroxy complexes are apparently present in a number of forms; some of the proposed hydrolysis products are $Al(OH)_2^{+}$, $Al(OH)^{2+}$, $Al(OH)_3$, $(Al_2(OH)_2)^{4+}$, and $(Al_{13}(OH)_{32})^{7+}$. Polymeric chain and ring structures form and, because of their large size and charge,

are non-exchangeable. OH:aluminum ratios of reported hydroxy interlayers vary widely, but are usually in the range 2.5 to 3 [27,28]. Those with OH:aluminum > 3 have often been observed to be unstable with respect to gibbsite. Gibbsite formation has been found to be favoured if sufficient aluminum is present to form more than half a complete gibbsite sheet for each montmorillonite sheet (about 8 g/kg) [29]. However, interlayer aluminum hydroxy complexes have been observed to control aluminum solubility in montmorillonite suspensions having a wide range of OH:aluminum ratio and total aluminum content [27]. Such complexes do not necessarily fill the entire interlayer space. Dixon and Jackson [30] reported X-ray evidence of significant interlayering in soils, for which they calculated that only 14% of the interlayer was filled. Small amounts of hydroxy polymers may concentrate at the edges of particles (see also the description by Pusch of iron hydroxide coatings on clays [31]), or be randomly dispersed in "islands" throughout the interlayer space.

Aluminum hydroxy interlayers in montmorillonite have been synthesized using a variety of techniques, such as precipitating hydroxides in the presence of clays [32] and reacting clays with aluminum hydroxide solutions [33,34]. They are commonly observed in soils, particularly mildly acid soils [35], and have been observed in sediments. A large number of ions can form such hydroxy interlayers. Magnesium hydroxy compounds are stable only in alkaline systems [34]. Fe^{2+} compounds have been observed under reducing conditions [36]. The very low solubility of $Fe(OH)_3$ limits the availability of Fe^{3+}, except in very acid systems.

The obvious question is why such interlayers have not been reported in similar studies of hydrothermal reactions involving smectite. There are a number of possible explanations:

(1) Much of the experimental work on smectite stability to date has been at temperatures from 250 to 400°C. At such temperatures, reaction kinetics are sufficiently accelerated that reactions involving lattice transformations dominate.

(2) In this study, the solid to solution ratio was low - 1:50 by weight. The experiments of Eberl and his co-workers all involved solid to solution ratios of 1:1 by weight. The 50-fold decrease in our case likely had a very large effect, since the extent of Al^{3+} hydrolysis depends on solution concentration [37]. In dilute solutions, Al^{3+} hydrolysis is much enhanced.

(3) A third possibility is simply that the presence of hydroxy interlayers has been missed previously. A 1.4-nm component in glycol- or glycerol-solvated samples of a complex clay mineral assemblage can be interpreted as chlorite, the second-order reflection of a 1.0 + 1.8 nm phase, or highly charged smectite (vermiculite). Hydroxy interlayers can only be positively identified by the re-expansion of the smectite after their removal. Reaction products from the experiments of both Roberson and Lahann (Figures 1 and 2 in [9]) and Inoue (Figure 5(f) in [6]) displayed peaks or peak shoulders around 1.4 nm in glycol-saturated samples. These may be due to aluminum hydroxy interlayers.

The formation of aluminum hydroxy interlayers in smectites has not been commonly reported for shales. It is, however, quite widespread in soils, and the clays in a backfilled nuclear waste disposal vault, being unlithified and uncemented, will bear some resemblance to a soil system. The lower permeability of shales may limit the availability of water, preventing the hydrolysis of Al^{3+}. Alternatively, higher temperatures during shale diagenesis may promote reactions that obscure the formation of aluminum hydroxy interlayers. Moreover, groundwater pH values are often lower in soils than in shale systems, due to dissolved CO_2.

It is difficult to assess the significance of this reaction for clay buffer materials in a nuclear waste disposal vault. Aluminum hydroxy interlayer formation is favoured by

- pH values in the range 4 to 6

- moderate aluminum availability
- low organic matter (organic matter may complex aluminum and retard the reaction) [28]
- wetting and drying cycles.

The reaction does not require elevated temperatures, since it is commonly observed in soil profiles. However, it will obviously proceed at temperatures up to 275°C under appropriate conditions. There would undoubtedly be enough aluminum available in a backfilled nuclear waste vault to form aluminum hydroxy interlayers. A smectite with a cation exchange capacity of 1 mcl(+)/kg requires only 3% gibbsite in the clay to provide sufficient aluminum to fill all the exchange sites. Very few clays are free of aluminum hydroxide and oxyhydroxide impurities. In addition, if crushed rock is used as a filler, dissolution of feldspar could provide a source of aluminum.

Although aluminum is available, its abundance relative to sodium and calcium is low in the saline brines representative of Canadian Shield groundwaters. McBride and Bloom [26] have demonstrated the inhibiting effect of Ca^{2+} in solution on Al^{3+} uptake by smectites, and it may be that high Ca^{2+} activity could swamp the selectivity for trivalent ions over divalent.

The pH conditions in the disposal vault will be of considerable importance. Smectites buffer the pH in the mildly alkaline region at ambient temperature over short time periods, but a sharp drop in pH (measured at 25°C) after treatment at temperatures above 150°C has been reported in hydrothermal studies of smectites, and a slower decrease at 30°C (see Section 4.1). At this stage, the possibility of establishing a low pH value in the vault cannot be ruled out.

The evidence presently available does not indicate unequivocally that cementation of buffer smectites by aluminum hydroxy interlayers will occur, but the possibility of such a reaction cannot be excluded. It is particularly significant in that it does not require elevated temperatures,

but will proceed at 25°C or less in a mildly acid groundwater. The potential effects on the physical and chemical properties are significant: swelling properties will be lost, since d_{001} is fixed at 1.4 nm; cation exchange capacity will be decreased both by occupancy of the exchange sites and by steric blocking of the exchange sites, due to the large size of the hydroxyl polymers; ion selectivity may also be affected [28], altering the sorption behaviour of the radionuclides. It is felt that further study of the reaction, particularly at high solid:solution ratios, is warranted.

4.3 ZEOLITES

The production of zeolites from clays at 200 and 275°C in alkaline systems is to be expected, since these are conditions commonly used in hydrothermal synthesis of zeolites for commercial purposes. Aiello and Franco [38] synthesized a variety of zeolites from montmorillonite at 80°C, using NaOH and KOh solutions of 0.25 to 2 mol/L. Franco and Aiello [39] produced analcime- and phillipsite-type zeolites from halloysite at temperatures between 200 and 340°C. Barrer [20] presents an excellent review of zeolite chemistry and hydrothermal synthesis. The type of zeolite produced, from the multitude of structures and compositions observed, is a sensitive function of

- temperature
- pH
- silicon:aluminum ratio
- silicon:water ratio
- types and amounts of cations
- aluminum:(calcium + sodium + potassium) ratios
- history-dependent factors.

The more compact, less hydrous zeolites (e.g., analcime, phillipsite) are favoured at high temperatures. Although a great variety of substitutions occurs, some cations favour particular structures (see Table 8). Co-crystallisation of several species is quite common. Further

complications are introduced by the tendency of zeolites to form metastable phases that gradually transform to more stable products (Ostwald's Rule).

The laboratory synthesis of zeolites usually involves very alkaline systems, since increasing alkalinity greatly increases the rates of nucleation and crystal growth of zeolites. Dayhurst and Sand [40] found that, for sodium potassium phillipsites at 100°C, nucleation time varied with $[OH^-]^2$ and crystallisation time with $[OH^-]^{1.75}$. Temperature has a greater effect on reaction kinetics. Activation energies for zeolite synthesis are around 60 kJ/mol (from 40 to 80 kJ/mol) [36]. Thus, the absence of zeolites in the experiments at 150°C and moderately alkaline pH (Run 4) may be due to kinetic effects rather than thermodynamic instability.

Neither high temperatures nor extremes of alkalinity are required to produce zeolites in geological systems where longer time spans are available. Zeolites occur in a variety of low-temperature environments, including geothermal areas and burial metamorphism of marine and lacustrine sediments.

Browne [41] reviewed the formation of zeolites via hydrothermal alteration in geothermal fields, and found that zeolites are abundant even at temperatures as low as 50°C, and persist to 350°C. Complex mineral assemblages and zonations are frequently observed, due to variations in temperature and composition of the hydrothermal solutions. In the calcic zeolites, for example, there is a tendency for zonation with increasing temperature, from mordenite (50°C) to laumontite and heulandite (100 to 150°C) to wairakite (175 to 200°C) [42,43]. Kristmannsdottir and Tomasson [44] have described similar temperature zonation in Icelandic geothermal fields, as shown in Figure 8. Zeolites are most common as alteration products of glass in volcanic rocks or their sedimentary derivates (including bentonites).

Hay [45] reviewed the occurrence of zeolites in sediments. A wide variety of zeolites, including analcime, phillipsite, faujasite,

natrolite and mordenite, are found in sediments from saline, alkaline lakes. These lakes are often characterized by bicarbonate-rich waters with pH = 9 to 10. However, phillipsite was reported as the principal authigenic silicate in sediments from a chloride-dominated lake in Teels Marsh, Nevada [42]. Zeolites are also abundant in marine and fresh-water sediments. Although they are most commonly reported in sediments of volcanic origin, they are found as cements, or replacing primary mineral phases or the clay matrix, in non-tuffaceous sediments. Zeolites are commonly associated with smectites, illite, or mixed-layer clays. Kastner [46] found that zeolites were abundant in deep-sea sediments, particularly phillipsite (found at the sediment-water interface) and clinoptilolite (found only at depth). Both were common in non-volcanic and volcanic clayey sediments, coexisting with smectite, opal, quartz and potassium feldspar. Kerr [47] reports the occurrence of clinoptilolite and heulandite with montmorillonite as products of the diagenesis of bentonites of marine origin, at a burial depth of about 3500 m (i.e., T = 100°C). Deffreyes [48] found clinoptilolite associated with potassium feldspar and montmorillonite in lacustrine vitric tuffs. Although they are commonly observed in close association, examples of phyllosilicates as obvious precursors of zeolites are rare, and zeolites usually appear to have formed at the expense of minor components (feldspars, amorphous material) in the clays.

As in laboratory synthesis, natural zeolites display abundant evidence of metastability and transformation of one phase to another. This may be initiated in part by structural modification caused by cation exchange. Hoss and Roy [49] observed substantial modification of zeolite frameworks due to cation exchange in the range 25 to 80°C. The tendency for metastable crystallisation is illustrated by the decreasing abundance of phillipsite, clinoptilolite, erionite and chabazite in rocks of increasing age from late Pleistocene to Eocene, while analcime increases proportionately [45].

Zeolites are favoured over clay mineral assemblages by

- high pH
- low partial pressure of CO_2 (i.e., high pH due to OH^- rather than bicarbonate; at high partial pressures of CO_2, calcite-clay assemblages form [50]).
- high silica activity
- high activity of sodium, potassium and calcium
- low total pressure (since they have low-density, open frameworks)
- closed systems (restricted groundwater flow) [37]

All these conditions, except high pH, are expected to occur in a nuclear waste disposal vault, in the presence of saline groundwater. Zeolite formation from glassy starting materials at moderately alkaline pH (8 to 10) is very common, but the available evidence suggests that zeolite formation from clay mineral precursors is inhibited except when the pH is sufficently high to promote dissolution of the phyllosilicate framework. As discussed previously, the question of groundwater pH in the buffer material is unresolved, but the possibility of high pH exists, especially in the event of extensive use of concrete for grouting, seals and bulkheads. At 50 to 150°C, low-temperature hydrous zeolites such as heulandite, stilbite, erionite and clinoptilolite are more likely to be formed than the higher temperature phases produced in our experimental runs, although both analcime and phillipsite are found at quite low temperatures in natural systems.

Zeolites are very efficient cation exchangers, having cation exchange capacities even greater than smectites (up to 6 mol(+)/kg); therefore, their formation is unlikely to decrease the cation exchange capacity of the buffer. However, the exchange properties of zeolites are highly dependent on cation size and, therefore, ion selectivities of the buffer may change considerably. Zeolites have open, low-density frameworks so that the transformation would not result in large volume decreases. They have no swelling properties, are brittle framework silicates, and are

often found as cements. Thus, zeolite formation could reduce the plasticity and swelling capacity of the buffer. The effect of zeolitization on buffer performance is discussed in more detail by Johnston and Miller [51].

4.4 FELDSPARS

Feldspars are commonly considered to be high-temperature minerals, but the alkali feldspars are stable over a wide range of conditions and their formation in low-temperature hydrothermal experiments is not unusual [20]. Sanidine has been synthesized from alkaline aluminosilicate gels at 150°C [52] and from albite at 175°C [53]. Potassium feldspars synthesized at low temperatures generally have the disordered lattice geometry observed in high-temperature feldspars.

Feldspars are common authigenic phases in both marine [46] and fresh-water [45] sediments. Albite is not common in post-Eocene sediments and is restricted almost entirely to depths of burial greater than 3500 m (i.e., temperatures above 100°C). Potassium feldspar is more widespread, but increases in abundance in rocks of increasing age. It is usually a relatively minor component, but Weiss [54] described an Ordovician bentonite tuff in which authigenic feldspar comprised more than 80% of the rock.

Both clays and zeolites transform to feldspars with increasing temperature. The reaction

analcime + quartz → albite + water

is taken as the boundary between diagenesis and low-temperature metamorphism [55]. Highly saline solutions stablilize feldspar. Campbell and Fyfe [56] found that the equilibrium temperature for the above reaction could be lowered from 190°C in distilled water to 65°C in saturated NaCl solution. Analcime is replaced by alkali feldspar at 50 to 75°C in highly saline groundwaters in the Green River Formation of Wyoming [45].

In general, it appears that appreciable albite formation requires both temperatures well in excess of 100°C and long periods of time (millions of years), and is unlikely to be important in a nuclear waste disposal vault. Saline groundwaters of the Canadian Shield are much richer in calcium than in sodium and so are more likely to stabilize calcium zeolite than albite. The kinetics of potassium feldspar formation are less sluggish, but potassium feldspar requires either high silica activity and moderate $K^+:H^+$ ratios or lower silica activity and high $K^+:H^+$ ratios. The activity of K^+ in Shield groundwaters is very low, and it is unlikely that potassium feldspar will form in significant amounts as an alteration product of bentonite buffer materials.

4.5 CLAY MINERALS

The main clay mineral reaction observed in the experimental runs was the transformation of smectite to illite or mixed-layer illite-smectite. Enhanced illite production in samples with a high final pH is attributed to the increased mobility of both aluminum and silicon at high pH, allowing transformation via a dissolution-reprecipitation mechanism. For samples in which the final pH was low, the only effect on the clay structure was the development of a slight beidellitic-layer charge. This is predicted as one of the steps in the slow transformation of smectite to illite [57].

The smectite-illite conversion has been discussed in detail elsewhere [31,58,59,60] and will not be reviewed here. The general consensus is that the transformation of smectite to illite is almost certain to occur at pH = 6 to 9 and temperatures above 100°C. However, the rate is strongly dependent on potassium availability and on the $K^+:(Na^+ + Ca^{2+})$ ratio. Some K^+ will be available in a nuclear waste disposal vault, particularly from dissolution of potassium feldspar if a crushed granitic filler is used in the buffer. However, in Shield brines, Ca^{2+} and Na^+ contents are so high that reaction rates will be slowed appreciably. The possible extent and effects of this reaction are assessed elsewhere [51].

4.6 EQUILIBRIUM THERMODYNAMIC CALCULATIONS

Theoretical equilibrium thermodynamic calculations can be applied to clay-mineral systems, but little reliable data on the standard thermodynamic properties of clay minerals are available. Even where end-member compositions are well characterized, it is difficult to assess the effects of the great variety of substitutions typical of clay minerals, and of entropy effects due to stacking disorder. Further complications are introduced by the tendency towards metastability at low temperatures. It is doubtful whether most low-temperature systems attain more than local equilibrium. However, thermodynamic stability diagrams are useful for predicting broad patterns of relative mineral stability and reaction trends under varying conditions.

The mineral stability diagrams of Helgeson et al. [61] for the systems SiO_2-Al_2O_3-Na_2O-K_2O-HCl (see Figure 9) and SiO_2-Al_2O_3-CaO-Na_2O-HCl (see Figure 10) show that increasing (i) sodium, potassium or calcium activity, (ii) pH, (iii) silica activity, or (iv) temperature will move a given system out of the domain of clay-mineral stability towards that of feldspars or zeolite. (Leonhardite is a calcium zeolite, $Ca_2Al_4Si_8O_{24}.7H_2O$.) The diagrams are calculated for equilibrium with respect to either quartz (lower silica activity) or amorphous silica.

The effect of alkali activity is particularly significant in view of the highly saline groundwaters found at depth in the Canadian Shield. Compositions for a typical, dilute, Na-Cl granite groundwater (GGW) and a saline, Ca-Na-Cl brine (SCSSS) are plotted on Figures 9 and 10. (Both are synthetic groundwater compositions taken from Sargent [62]; pH = 6.5 for GGW; pH = 7.0 for SCSSS.) On the sodium-potassium diagrams (Figure 9), the GGW falls within the clay-mineral stability field under all conditions of interest. Increased Na^+ activity in the brine is sufficient to shift it into the feldspar stability field at higher temperature or silica activity. For the calcium-sodium diagrams (Figure 10), Ca^{2+} activity in the SCSSS is sufficiently high that it falls in the stability field of the zeolite leonhardite regardless of temperature and silica activity. Even the GGW is

in equilibrium with clays only at the lowest temperature and silica activity.

These diagrams are not sufficiently accurate to be used to predict stable mineral assemblages. (For instance, they predict no smectite-quartz coexistence at 25°C.) However, they do reinforce the argument that zeolites and feldspars become increasingly stable in low-temperature systems as pH, silica activity or temperature increases, particularly in the presence of concentrated saline solution.

5. CONCLUSIONS

At moderate pH and temperatures of 50 to 150°C, the most important reaction affecting smectite stability is the transformation to illite. However, both geological and experimental evidence indicate that elevated groundwater pH could induce the production of zeolites and/or feldspars. At temperatures up to 150°C, zeolites are the more likely reaction products, since feldspar crystallisation kinetics are very slow at low temperatures.

In the mildly acidic region, little modification of the smectite framework occurs in the temperature range 50 to 150°C, except in the presence of excess K^+. Fixation of aluminum hydroxy species in the interlayer spaces can occur without structural modification at low temperatures, reducing both the swelling and cation exchange capacities of the smectite.

Shifts in pH to either the alkaline or acidic region can impose different sets of reactions for smectites. In both cases, the effects on the physical and chemical properties of a smectite-based buffer would be profound. Until the pH conditions prevailing in a nuclear waste disposal vault can be predicted with confidence, these reactions must be considered in assessing changes in buffer performance due to interaction of the buffer with groundwater.

ACKNOWLEDGEMENTS

We wish to thank M. Duclos and J. Snider for their assistance in providing X-ray diffraction analyses, Professor Armin Weiss (Universität München), who suggested the presence of aluminum hydroxy interlayers in the experimental reaction products, and R.B. Heimann and D.W. Oscarson for constructive review of the manuscript.

REFERENCES

1. G.W. Bird and D.J. Cameron, "Vault Sealing Research for the Canadian Nuclear Fuel Waste Management Program," Atomic Energy of Canada Limited Technical Record, TR-145* (1982).

2. D.W. Oscarson and S.C.H. Cheung, "Evaluation of Phyllosilicates as a Buffer Component in the Disposal of Nuclear Fuel Waste," Atomic Energy of Canada Limited Report, AECL-7812 (1983).

3. D.D. Eberl, "Reaction Series for Dioctahedral Smectites," Clays Clay Miner. 26, 327 (1978).

4. D.D. Eberl and J. Hower, "The Hydrothermal Transformation of Sodium and Potassium Smectite into Mixed-Layer Clay," Clays Clay Miner. 25, 215 (1977).

5. D.D. Eberl, "The Reaction of Montmorillonite to Mixed-Layer Clay: The Effect of Interlayer Alkali and Alkaline Earth Cations," Geochim. Cosmochim. Acta 42, 1 (1978).

6. A. Inoue, "Potassium Fixation by Clay Minerals during Hydrothermal Treatment," Clays Clay Miner. 31, 81 (1983).

7. S. Komarneni and W.B. White, "Hydrothermal Reactions of Strontium and Transuranic Simulator Elements with Clay Minerals, Zeolites and Shales," Clays Clay Miner. 31, 113 (1983).

8. S. Komarneni and W.B. White, "Hydrothermal Reaction of Clay Minerals and Shales with Cesium Phases from Spent Fuel Elements," Clays Clay Miner. 29, 299 (1981).

9. H.E. Roberson and R.W. Lahann, "Smectite to Illite Conversion Rates: Effects of Solution Chemistry," Clays Clay Miner. 29, 129 (1981).

10. R.M. Quigley, "Quantitative Mineralogy and Preliminary Pore-Water Chemistry of Candidate Buffer and Backfill Materials for a Nuclear Fuel Waste Disposal Vault," Atomic Energy of Canada Limited Report, AECL-7827 (1984).

11. H.G. Miller, "Preparation of Clay Minerals for X-ray Diffraction Analysis," Whiteshell Nuclear Research Establishment Report, WNRE-604 (1984).

12. R. Greene-Kelly, "The Identification of Montmorillonoids in Clays," J. Soil Sci. 4, 233 (1953).

13. D.M.C. MacEwan and M.J. Wilson, "Interlayer and Intercalation Complexes of Clay Minerals," in Mineralogical Society Monograph No. 5, Crystal Structures of Clay Minerals and their X-ray Identification, G.W. Brindley and G. Brown (eds.), Miner. Soc: London, 1980.

14. R.C. Reynolds, "Interstratified Clay Minerals," in Mineralogical Society Monograph No. 5, Crystal Structures of Clay Minerals and their X-ray Identification, G.W. Brindley and G. Brown (eds.), Miner. Soc: London, 1980.

15. J. Srodon, "Precise Identification of Illite-Smectite Interstratifications by Powder X-ray Diffraction," Clays Clay Miner. 28, 401 (1980).

16. J. Hower, "X-ray Identification of Mixed-Layer Clay Minerals," in Short Course in Clays and the Resource Geologist, F.J. Longstaffe (ed.), Miner. Assoc. Canada, 1981.

17. A. Weiss, private communication, 1983.

18. R.A. Gubser and F. Laves, "X-ray Properties of Adularia $(K,Na)AlSi_3O_8$," Schweiz, Mineral Petrog. Mitt. 47, 177 (1967).

19. F. Aumento, "Thermal Transformations of Selected Zeolites and Related Hydrated Silicates," Ph. D. Thesis, Dalhousie University, Halifax, Nova Scotia (1967).

20. R.M. Barrer, Hydrothermal Chemistry of Zeolites, Academic Press, London 1982.

21. D.D. Eberl, G. Whitney and H.N. Khoury, "Hydrothermal Reactivity of Smectite," Amer. Mineral. 63, 401 (1978).

22. E. Galli and A.G. Loschi Ghittoni, "Crystal Chemistry of Phillipsites," Amer. Mineral. 57, 1125 (1972).

23. R.E. Grim, Clay Mineralogy, 2nd edition, McGraw-Hill, New York, 1968.

24. Z. Gerstl and A. Banin, "Fe^{2+}-Fe^{3+} Transformations in Clay and Resin Ion-Exchange Systems," Clays Clay Miner. 28, 335 (1980).

25. J.L. Bischoff and W.E. Seyfried, "Hydrothermal Chemistry of Seawater from 25°C to 350°C," Amer. J. Sci. 278, 838 (1978).

26. M.B. McBride and P.R. Bloom, "Adsorption of Aluminum by a Smectite: II An Al^{3+}-Ca^{2+} Exchange Model," Soil Sci. Soc. Amer. J. 41, 1073 (1977).

27. P.R. Bloom, M.B. McBride and B. Chadbourne, "Adsorption of Aluminum by a Smectite: I. Surface Hydrolysis During Ca^{2+}-Al^{3+} Exchange," Soil Sci. Soc. Amer. J. 41, 1068 (1977).

28. C.I. Rich, "Hydroxy Interlayers in Expansible Layer Silicates," Clays Clay Miner. 16, 15 (1968).

29. R.C. Turner and J.E. Brydon, "Effect of Length of Time of Reaction on Some Properties of Suspensions of Arizona Bentonite, Illite, and Kaolinite in Which Aluminum Hydroxide is Precipitated," Soil Sci. 103, 111 (1967).

30. J.B. Dixon and M.L. Jackson, "Properties of Intergradient Chlorite-Expansible Layer Silicates of Soils," Soils Sci. Soc. Amer. Proc. 26, 358 (1962).

31. R. Pusch, "Stability of Deep-sited Smectite Minerals in Crystalline Rock," KBS TR 83-16 (1983).

32. M. Slaughter and I.H. Milne, "The Formation of Chlorite-like Structures from Montmorillonite," in Clays and Clay Minerals, Proc. 7th Natl. Conf. held in 1958, Pergamon Press, New York, 1960, p. 114.

33. C.I. Rich, "Aluminum in Interlayers of Vermiculite," Soil Sci. Soc. Amer. Proc. 24, 26 (1960).

34. D.D. Carstea, "Formation and Stability of Aluminum, Iron and Magnesium Interlayers in Montmorillonite and Vermiculite," unpublished Ph.D. thesis. Oregon State University, Corvallis, Oregon (1967).

35. M.L. Jackson, "Clay Transformation in Soil Genesis During the Quarternary," Soil Sci. 99, 15 (1965).

36. W.C. Lynn and L.D. Whittig, "Alteration and Formation of Clay Minerals During Cat Clay Formation," Clays Clay Miner. 14, 241 (1964).

37. R.W. Smith, "Relations Among Equilibrium and Non-equilibrium Aqueous Species of Aluminum Hydroxy Complexes," in Non-equilibrium Systems in Natural Water Chemistry, Advances in

Chemistry Series 106, American Chemical Society, Washington, D.C. 1971, p. 250.

38. R. Aiello and E. Franco, "Formation of Zeolites by Transformation of Halloysite and Montmorillonite at Low Temperature in Alkaline Environments", Rend Accad. Sci. Fis. Mat., Naples 35, 165 (1968).

39. E. Franco and R. Aiello, "Zeolitization of Natural Glasses, Rend Accad., Sci., Fis. Mat., Naples 36, 174 (1969).

40. D.T. Hayhurst and L.B. Sand, in Molecular Sieves II (ed. J.R. Katzner), Amer. Chem. Soc. Symp. Ser. 40, 219 (1977).

41. P.R.L. Browne, "Hydrothermal Alteration in Active Geothermal Fields," Annu. Rev. Earth Planet. Sci. 6, 229 (1978).

42. P.R.L. Browne and A.J. Ellis, "The Ohaki-Broadlands Hydrothermal Area, New Zealand: Mineralogy and Related Geochemistry," Amer. J. Sci. 269, 97 (1970).

43. Y. Seki, H. Onuki, K. Okumura and I. Takashima, "Zeolite Distribution in the Katayama Geothermal Area, Onikobe, Japan," Jpn. J. Geol. Geogr. Trans. 40, 63 (1969).

44. H. Kristmansdottir and J. Tomasson "Zeolite Zones in Geothermal Areas in Iceland," in Natural Zeolites: Occurrence, Properties, Use, L.B. Sand and F.A. Mumpton (eds.), Pergamon Press, Oxford, 1978, pp. 277-284.

45. R.L. Hay, "Zeolites and Zeolitic Reactions in Sedimentary Rocks," GSA Special Paper 85 (1966).

46. M. Kastner, "Authigenic Silicates in Deep-sea Sediments: Formation and Diagenesis," in The Oceanic Lithosphere (C. Emiliani, ed.) in the collection The Sea, Ideas and Observations on Progress in the Study of the Seas, John Wiley and Sons, New York, NY, 1981, Vol.7, pp. 915-980.

47. P.F. Kerr, "Bentonite from Ventura, California," Econ. Geol. 26, 153 (1931).

48. K.S. Deffreyes, "Zeolites in Sedimentary Rocks," J. Sed. Petrol. 29, 602 (1959).

49. H. Hoss and R. Roy, "Zeolite Studies III: On Natural Phillipsite, Gismondite, Harmotome, Chabazite and Gmelinite." Beitr. Mineral. U. Petrol. 7, 389 (1960).

50. A.B. Thompson, "P_{CO_2} in Low-grade Metamorphism: Zeolite, Carbonate, Clay Mineral, Prehnite Relations in the System

$CaO-Al_2O_3-SiO_2-CO_2-H_2O$," Contrib. Mineral. Petrol. 33, 145 (1971).

51. R.M. Johnston and H.G. Miller, "Hydrothermal Stability of Bentonite-Based Buffer Materials in a Nuclear Waste Disposal Vault," Atomic Energy of Canada Report (in preparation).

52. R.M. Barrer and J.W. Baynham, "Hydrothermal Chemistry of the Silicates. VII Synthetic Potassium Aluminosilicates," J. Chem. Soc. 2882 (1956).

53. A. Erdem and L.B. Sand, "Metastable Phase Transformations and Morphological Changes of NA-, Na, K- and K-ZSM-5 with Salt Additions," in Proc. 5th. Int. Conf. Zeolite, Heyden, L.V.C. Reeves (ed.), London, 1980, pp. 64-72.

54. M.P. Weiss, "Feldspathized Shales from Minnesota," J. Sed. Petrol. 24, 270 (1954).

55. H.G.F. Winkler, Petrogenesis of Metamorphic Rocks, 5th edition, Springer Verlag, New York, 1979.

56. A.S. Campbell and W.S. Fyfe, "Analcime-Albite Equilibria," Amer. J. Sci. 263, 807 (1965).

57. L.G. Schultz, "Mixed-Layer Clay in the Pierre Shale and Equivalent Rocks, Northern Great Plains Region," USGS Prof. Paper 1064-A (1978).

58. R.M. Johnston, "The Conversion of Smectite to Illite in Hydrothermal Systems: A Literature Review," Atomic Energy of Canada Limited Report, AECL-7792 (1983).

59. D.M. Anderson, "Smectite Alteration," KBS TR 83-03 (1983).

60. D.M. Anderson, "Smectite Alteration II," (in preparation).

61. H.C. Helgeson, T.H. Brown and R.H. Leeper, Handbook of Theoretical Activity Diagrams Depicting Chemical Equilibria in Geologic Systems Involving an Aqueous Phase at one Atm. and 0° to $300^{\circ}C$, Freeman, Cooper and Co., San Francisco, 1969.

62. F.P. Sargent, "Applied Chemistry and Geochemistry Research for the Canadian Fuel Waste Management Program," Atomic Energy of Canada Limited Technical Report, TR-149* (1982).

* Unrestricted, unpublished report available from SDDO, Atomic Energy of Canada Limited Research Company, Chalk River, Ontario, KOJ 1JO.

TABLE 1

RESULTS OF RUN 1 AFTER 30 DAYS AT 275°C

Sample No.*	Interlayer Cation	Solution Composition	$pH_{initial}$	pH_{final}**	Reaction Products†
1.1	Ca	DDW	6.3	4	$S_G(1.8)$, Q
1.2	Ca	0.01 mol/L KCl	5.9	4	$S_G(1.8)$, Q
1.3	Ca	0.05 mol/L KCl	5.9	4	$S_G(1.8)$, Q
1.4	Ca	0.10 mol/L KCl	5.8	4	$S_G(1.8)$, I, Q
1.5	Ca	0.25 mol/L KCl	5.8	4	$S_G(1.8)$, $S_G(1.4)$, I, Q
1.6	Ca	0.50 mol/L KCl	5.8	4	$S_G(1.8)$, $S_G(1.4)$, I, Q
1.7	Ca	1.00 mol/L KCl	5.8	4	$S_G(1.8)$, $S_G(1.4)$, I, Q
1.8	Ca	0.1 mol/L $K^+(HCO_3^- + Cl^-)$ ††	7.7	8.5	Am, Ksp, S(1.2) - I, Q
1.9	Ca	1.0 mol/L $K^+(HCO_3^- + Cl^-)$ ††	8.3	9.5	Am, Ksp, S(1.2) - I, Q
1.10	Na	DDW			
1.11	Na	0.01 mol/L KCl	7.5	-	-
1.12	Na	0.10 mol/L KCl	6.5	3	$S_G(1.8)$, $S_G(1.4)$, I, Q
1.13	Na	0.50 mol/L KCl	7.8	3	$S_G(2.8)$, $S_G(1.8)$, I, Q
1.14	Na	0.10 mol/L $K^+(HCO_3^- + Cl^-)$ ††	8.6	10	Am, Ksp, S(1.2) - I, Q
1.15	Na	1.0 mol/L $K^+(HCO_3^- + Cl^-)$ ††	8.3	10	Am, Ksp, S(1.2) - I, Q

* 200 mg clay in 10 mg solution in stainless-steel Parr pressure vessels with Teflon liners

** Final pH measured at 25°C

† Q = quartz, I = illite, Ksp = potassium feldspar, Am = analcime, S(x) = smectite with d_{001} = x nm (RH = 52%), $S_G(x)$ = smectite with d_{001} = x nm (after glycerol saturation), DDW = deionized, distilled water

†† Bicarbonate buffer solution prepared with HCO_3^-:Cl^- = 3:2

TABLE 2

RESULTS OF RUN 2 AFTER 15 DAYS AT 275°C

Sample No.*	Interlayer Cation	$[OH^-]$ (mol/L)	$pH_{initial}$	pH_{final}**	Reaction Products†
2.1	Na	0.2	12.8	12.4	Ksp, Ph, Q, I
2.2	Na	0.1	12.6	-	water lost from sample
2.3	Na	0.075	12.5	11.6	Ksp, Q, I, S(1.2)
2.4	Na	0.050	12.3	7.8	Ksp, Q, I, S(1.2)
2.5	Na	0.025	12.0	4.5	Ksp, Q, I, S(1.2)
2.6	Na	0.010	11.7	3.1	S(12), I, Ksp, Q
2.7	Na	0.005	10.9	3.4	S(Al), I, Q
2.8	Na	0	8.4	3.2	S(Al), I, Q
2.9	Ca	0.2	12.9	12.4	Ksp, Ph, I, Q
2.10	Ca	0.1	12.6	11.8	Ksp, Ph, I, Q, S(1.2)
2.11	Ca	0.075	12.5	10.7	Ksp, I, Q, S(1.2)
2.12	Ca	0.050	12.2	6.6	Ksp, I, Q, S(1.2)
2.13	Ca	0.025	12.0	5.8	Ksp, I, Q, S(1.2)
2.14	Ca	0.010	11.5	5.9	S(1.2), I, Q
2.15	Ca	0.005	10.9	5.0	S(Al), I, Q
2.16	Ca	—	8.5	4.7	S(Al), I, Q, (Ksp)

* 50 mg clay in 2.5 g solution in sealed gold tube in an autoclave; $[K^+]$ = 0.1 mol/L as KOH + KCl

** Final pH measured at 25°C

† Symbols as for Table 1; Ph = phillipsite; S(Al) = 1.4-nm smectite with aluminum hydroxy interlayers

TABLE 3

RESULTS OF RUN 3 AFTER 27 DAYS AT 200°C

Sample No.*	Interlayer Cation	$[OH^-]$ (mol/L)	$pH_{initial}$	pH_{final}**	Reaction Products†
3.1	Na	0.1	12.6	12.4	Ksp, Ph, I, S(1.2), Q
3.2	Na	0.05	12.3	-	Ksp, I, S(1.2), Q
3.3	Na	0.025	12.0	-	S(1.2), I, Q
3.4	Na	0.010	11.7	5.7	S(Al, 1.4 > 1.8), I, Q
3.5	Na	0.005	10.9	5.0	S(Al, 1.4 ≈ 1.8), I, Q, Ksp
3.6	Na	0.002	10.7	-	S(Al, 1.4 < 1.8), I, Q
3.7	Na	0.001	10.6	4.4	S(Al, 1.4 ≈ 1.8), I, Q
3.8	Na	-	8.4	5.7	S(Al, 1.4 < 1.8), I, Q
3.9	Ca	0.1	12.6	12.5	Ph, Ksp, I, S(1.2), Q
3.10	Ca	0.05	12.4	-	Ksp, Ph, I, S(1.2), Q
3.11	Ca	0.025	12.0	8.2	Ksp, S(Al, 1.4 < 1.8), I, Q
3.12	Ca	0.010	11.7	5.6	Ksp, S(Al, 1.4 > 1.8), I, Q
3.13	Ca	0.005	10.8	5.2	S(Al, 1.4 ≈ 1.8), I, Q
3.14	Ca	0.002	10.8	5.0	S(Al, 1.4 > 1.8), I, Q
3.15	Ca	0.001	10.6	-	S(Al, 1.4 ≈ 1.8), I, Q
3.16	Ca	-	8.5	5.1	S(Al, 1.4 < 1.8), I, Q

* 50 mg clay in 2.5 g solution in sealed gold tube in an autoclave; $[K^+]$ = 0.1 mol/L as KOH + KCl

** Final pH measured at 25°C

† Symbols as for Table 2; S(Al, 1.4 ≈ 1.8) = smectite with aluminum hydroxy interlayers, in which the 1.4-nm and 1.8-nm peaks after glycerol saturation are of approximately equal intensity

TABLE 4

RESULTS OF RUN 4 AFTER 30 DAYS AT 150°C

Sample No. *	Interlayer Cation	$[OH^-]$ (mol/L)	$pH_{initial}$	pH_{final}**	Reaction Products †
4.1	Na	0.05	12.3	11.0	S(Al, 1.4 < 1.8), I, Q
4.2	Na	0.010	11.7	7.2	S(Al, 1.4 ≈ 1.8), I, Q
4.3	Na	0.0075	11.2	6.3	S(Al, 1.4 < 1.8), I, Q
4.4	Na	0.005	10.9	-	S(Al), I, Q
4.5	Na	0.001	10.6	6.2	S(Al, 1.4 > 1.8), I, Q
4.6	Na	0.0005	10.3	6.0	S(Al), I, Q
4.7	Na	0.0001	9.6	5.5	S(Al, 1.4 ≈ 1.8), I, Q
4.8	Na	0	8.4	5.6	S(Al, 1.4 ≈ 1.8), I, Q
4.9	Ca	0.05	12.3	10.1	S(Al, 1.4 ≈ 1.8), I, Q
4.10	Ca	0.010	11.7	7.1	S(Al, 1.4 ≈ 1.8), I, Q
4.11	Ca	0.0075	11.2	6.2	S(Al), I, Q
4.12	Ca	0.0050	10.9	5.2	S(Al), I, Q
4.13	Ca	0.0010	10.6	6.1	S(Al), I, Q
4.14	Ca	0.0005	10.3	6.4	S(Al, 1.4 > 1.8), I, Q
4.15	Ca	0.0001	9.6	6.3	S(Al), I, Q
4.16	Ca	0	8.5	5.2	S(Al, 1.4 > 1.8), I, Q

* 50 mg clay in 2.5 solution in sealed gold tube in an autoclave; $[K^+]$ = 0.1 mol/L as KOH + KCl

** Final pH measured at 25°C

† Symbols as for Tables 1 and 2

TABLE 5

BASAL SPACINGS OF SMECTITES [11]

Smectite	Relative Humidity 52% (nm)	Glycerol Procedure (nm)
Mg-montmorillonite	1.49 - 1.51	1.76 - 1.78
Mg-beidellite	1.47	1.76 - 1.78
Mg-vermiculite	1.44	1.43
Li-montmorillonite, heated to 300°C	0.95	0.95
Li-beidellite	0.95	1.77

TABLE 6

COMPARISON OF OBSERVED d-SPACINGS FOR SAMPLE 1.15 WITH XRPDF PATTERNS

Observed d-spacings (nm)	XRPDF 10-353* Synthetic High Sanidine[18]	XRPDF 7-363* Analcime[19]
1.1		
1.0		
0.67		0.688
0.591		
0.564		0.561
0.486		0.485
0.451		
0.425 Q	0.424	
0.396	0.395	
0.380	0.379	
	0.367	0.367/0.364 doublet
0.345	0.346	0.343
0.334 Q	0.332	
0.329 triplet	0.326 triplet	
0.324	0.322	
0.301	0.2995	0.308
0.2928	0.293/0.290 triplet	0.2929
		0.2896
0.2803		0.2804
0.2769	0.2766	
0.2696		0.2696
0.2605		0.2673
0.2590	0.2582	
0.2513		0.2506

* Only peaks with intensity I $\geq$ 20 are listed; those with I $\geq$ 80 are underlined. Quartz peaks are marked with a Q.

TABLE 7

COMPARISON OF OBSERVED d-SPACINGS FOR SAMPLE 2.1 WITH XRPDF PATTERNS

Observed d-Spacings (nm)	XRPDF 10-353* Synthetic High Sanidine [18]	XRPDF 12-195* Synthetic Phillipsite [22]	XRPDF 20-923 Phillipsite
0.95-1.0		0.95	
		0.82	
0.71		0.72	0.72
		0.70	
0.58		0.56	
0.534		0.54	
0.498		0.50	0.506
	0.468		
0.450 (broad)		0.450	
		0.434	
0.423 Q	0.424		0.413
0.395	0.395	0.403	
		0.388	
0.379	0.379		
0.362		0.358	
0.346	0.346	0.345	
0.342			
0.332 Q	0.332	0.335	
0.328 broad triplet	0.326		
0.322	0.322	0.324	0.326
0.314		0.319	0.319
0.300	0.2995		0.314
0.292	0.293/0.290 triplet	0.293	
0.284			
0.279			
0.276	0.2766	0.273	0.275
		0.268	0.2698
0.260		0.260	
0.258	0.2582		
0.252		0.251	

* Only peaks with intensity, I $\geq$ 20 are listed; those with I $\geq$ 80 are underlined. Quartz peaks are marked with a Q.

TABLE 8

ZEOLITE SYNTHESIS IN RELATION TO CATION TYPE [34]

Zeolite	Preferred Cation
Gismondine type	Na
Faujasite type	Na
Gmelinite type	Na
Analcime type	Various
Mordenite	Na, alkaline earth ions
Edingtonite type	K, Rb, Cs, Ba
Phillipsite type	K and others
Chabazite type	K
Thomsonite	Ca
Epistilbite	Ca

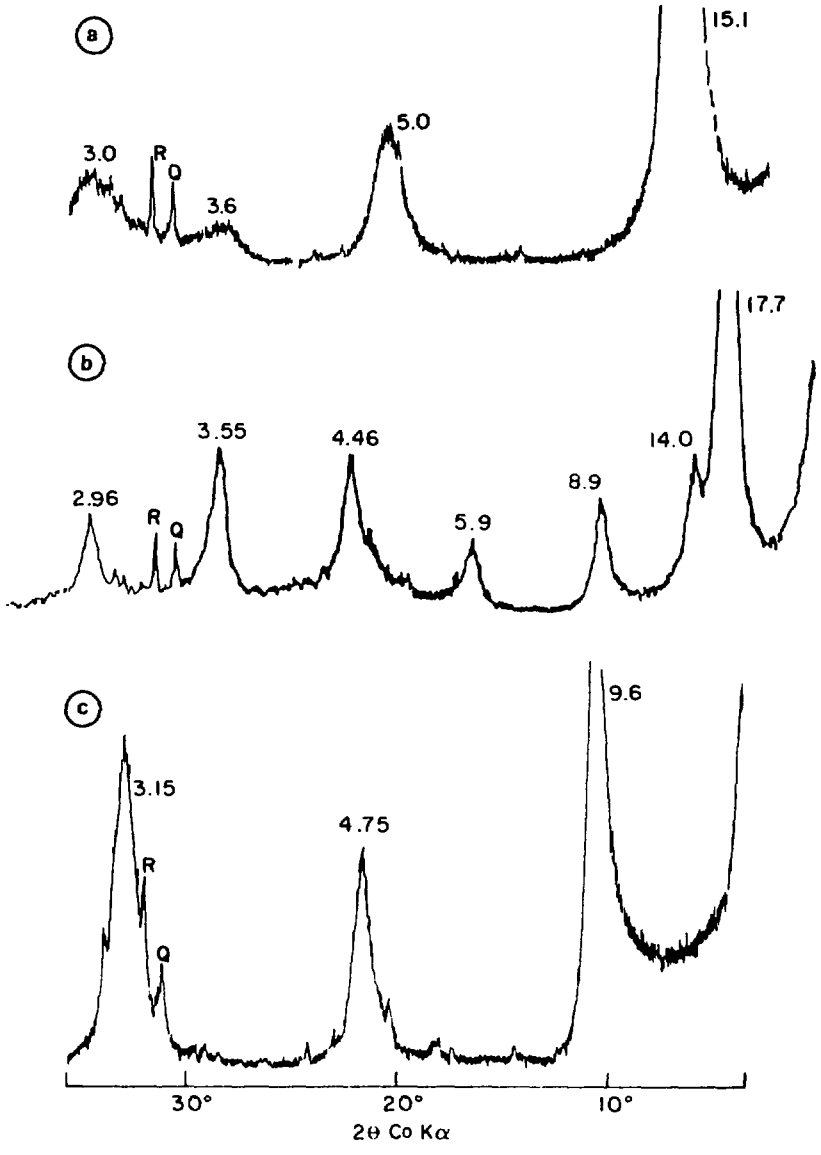

FIGURE 1: XRD Patterns for Filtaclay, <2 μm Fraction Used as Starting Material
(a) Magnesium-Saturated, 59% Relative Humidity
(b) Magnesium-Saturated, Glycerol Solvation
(c) Lithium-Saturated, Heated to 300°C, Glycerol Saturation
R = Rutile, Q = Quartz, Interplanar Spacings (nm x 10) Are Indicated for Diffraction Peaks.

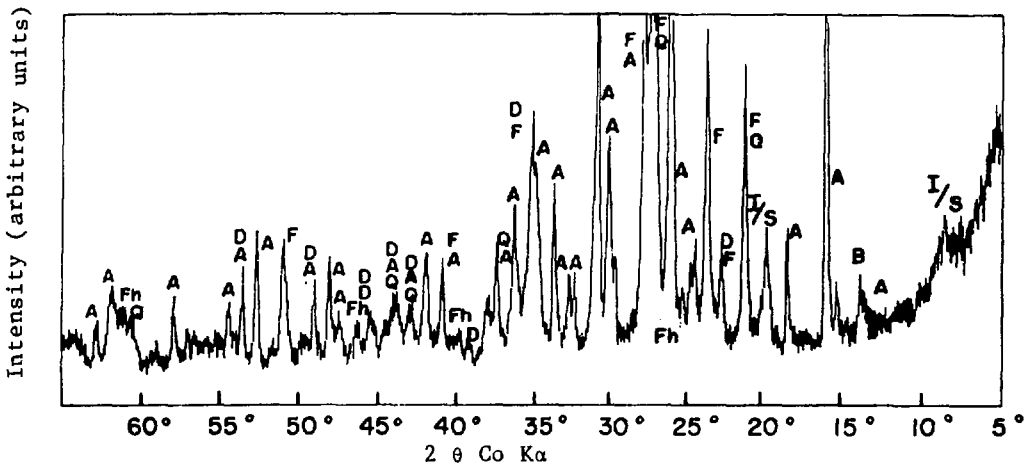

FIGURE 2: XRD Pattern for Sample 1.15:
A = Analcime/Wairakite; F = Feldspar; B = Boehmite; Q = Quartz; D = Diaspore; Fh = Ferrihydrite; I/S = Mixed-layer Illite/Smectite

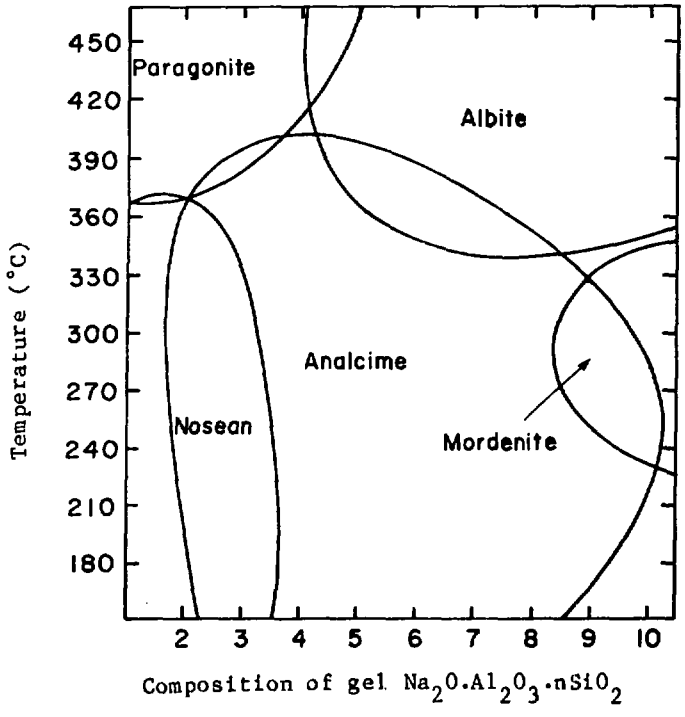

FIGURE 3: Stability Fields of Sodium-Zeolites (after Barrer [20])

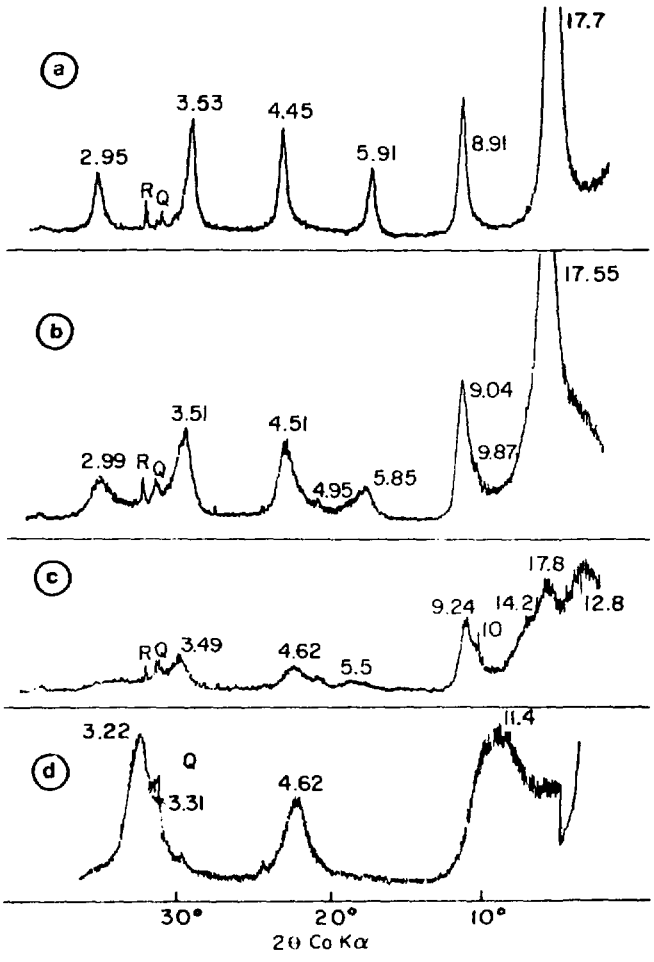

FIGURE 4: XRD Patterns for Samples from Run 1
(a) Sample 1.1, Magnesium-Saturated, Glycerol-Solvation
(b) Sample 1.6, Magnesium-Saturated, Glycerol-Solvation
(c) Sample 1.13, Magnesium-Saturated, Glycerol-Solvation
(d) Sample 1.6, Lithium-Saturated, Heated to 300°C, Glycerol Solvation
R = Rutile, Q = Quartz (Interplanar Spacings (nm x 10) Are Indicated.)

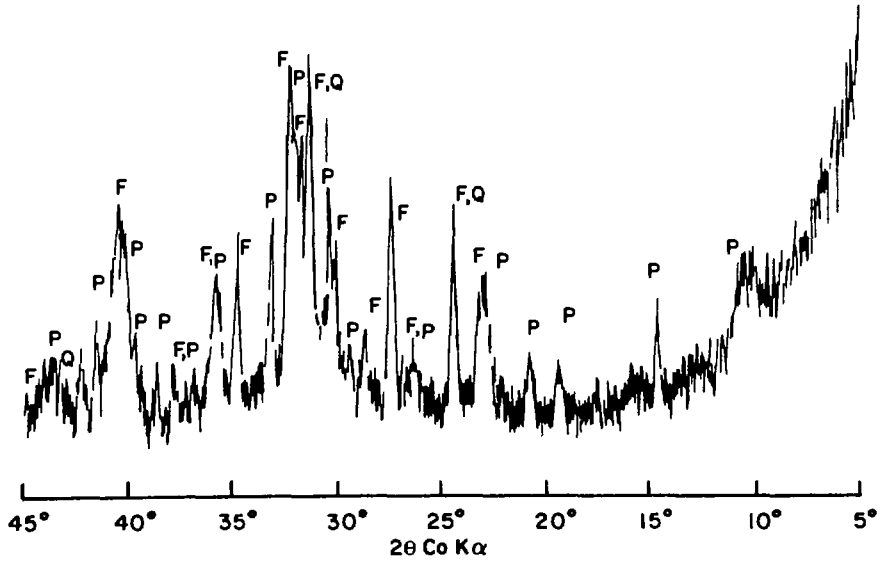

FIGURE 5: XRD Pattern for Sample 2.1:
P = Phillipsite; F = Feldspar (Sanidine); Q = Quartz.

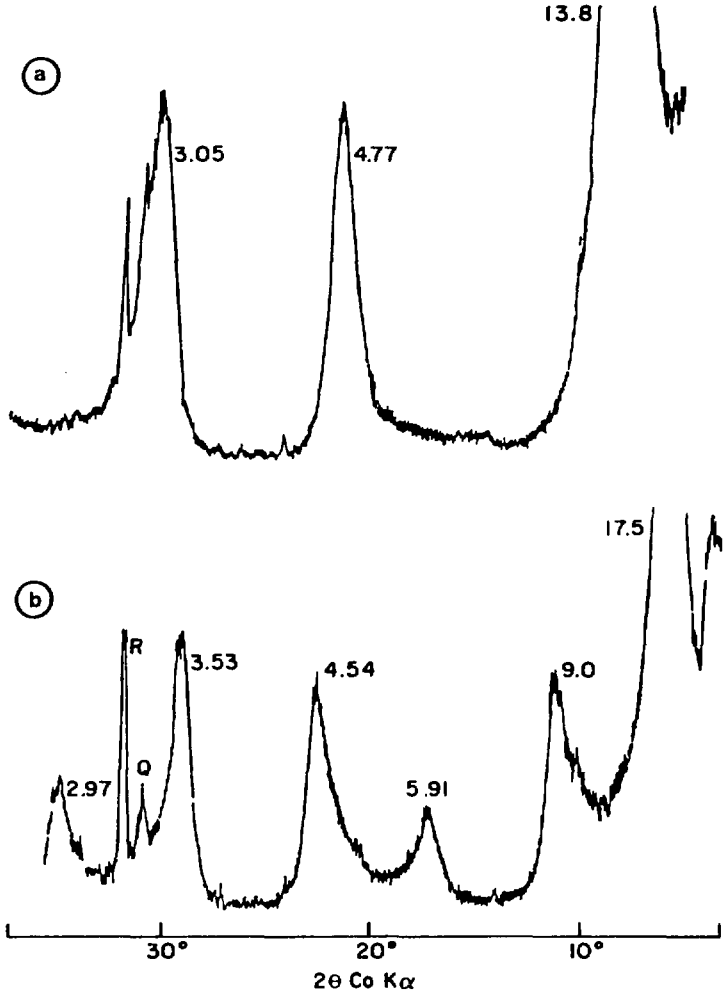

FIGURE 6: XRD Pattern for Sample 2.7 Showing Effect of Removal of Aluminum Hydroxy Interlayers (Interplanar spacings (nm x 10) Are Indicated.)
(a) Magnesium-Saturated, Glycerol Solvation
(b) Treated with Sodium Tartrate Followed by Magnesium-Saturated, Glycerol Solvation.

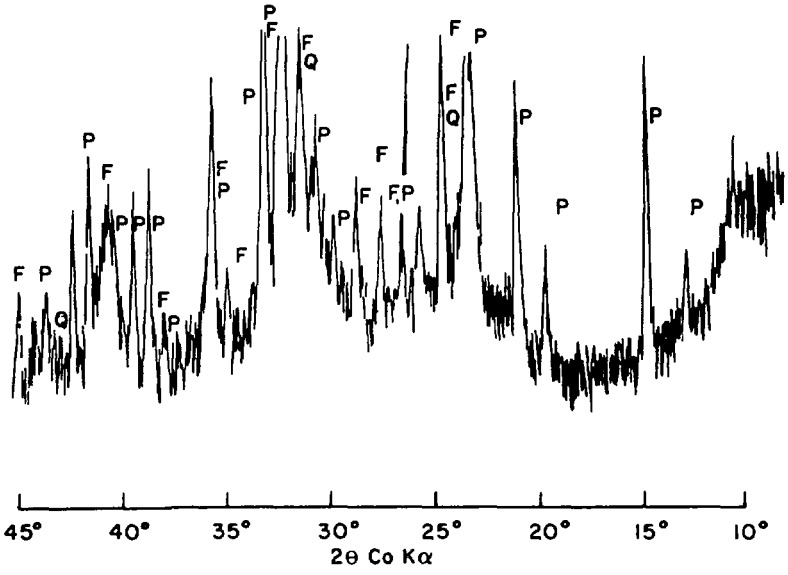

FIGURE 7: XRD Pattern for Sample 3.1; P = Phillipsite; F = Feldspar (Sanidine); Q = Quartz

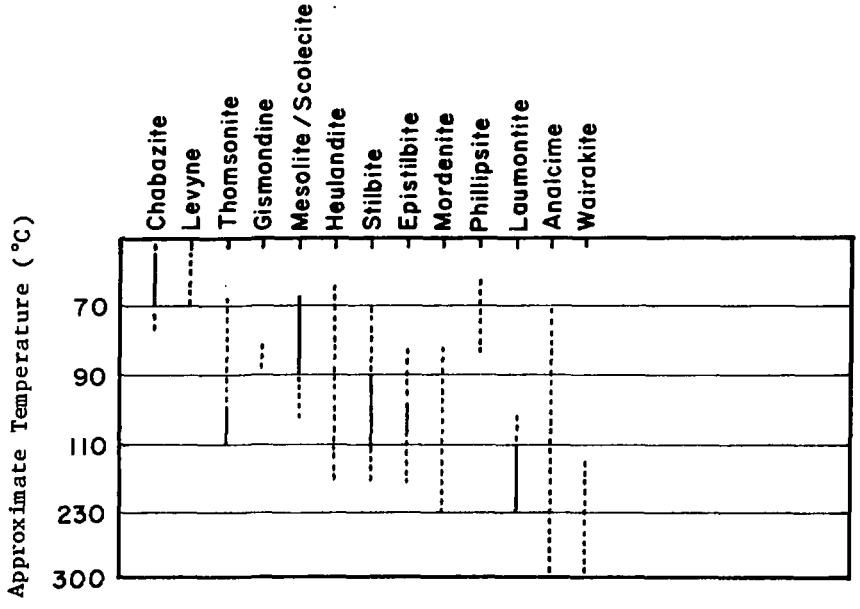

FIGURE 8: Temperature Zoning of Zeolites Occurring in Icelandic Geothermal Areas (after Kristmanssdottir and Tomasson [44])

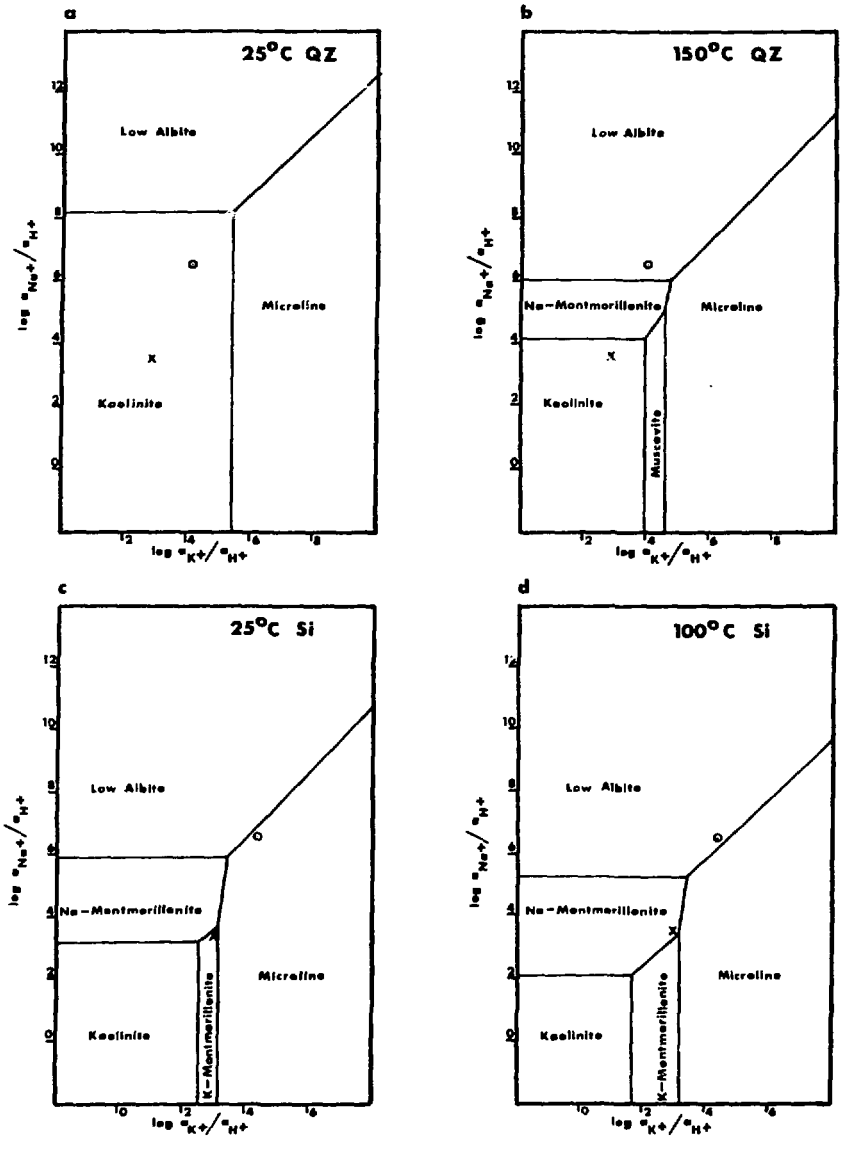

FIGURE 9: Theoretical Stability Fields in the System SiO_2-Al_2O_3-Na_2O-K_2O-HCl (after Helgeson et al. [61])

QZ = Quartz Saturation
Si = Amorphous Silica Saturation
o = Standard Canadian Shield Saline Solution (SCSSS)
x = Granite Groundwater (GGW)

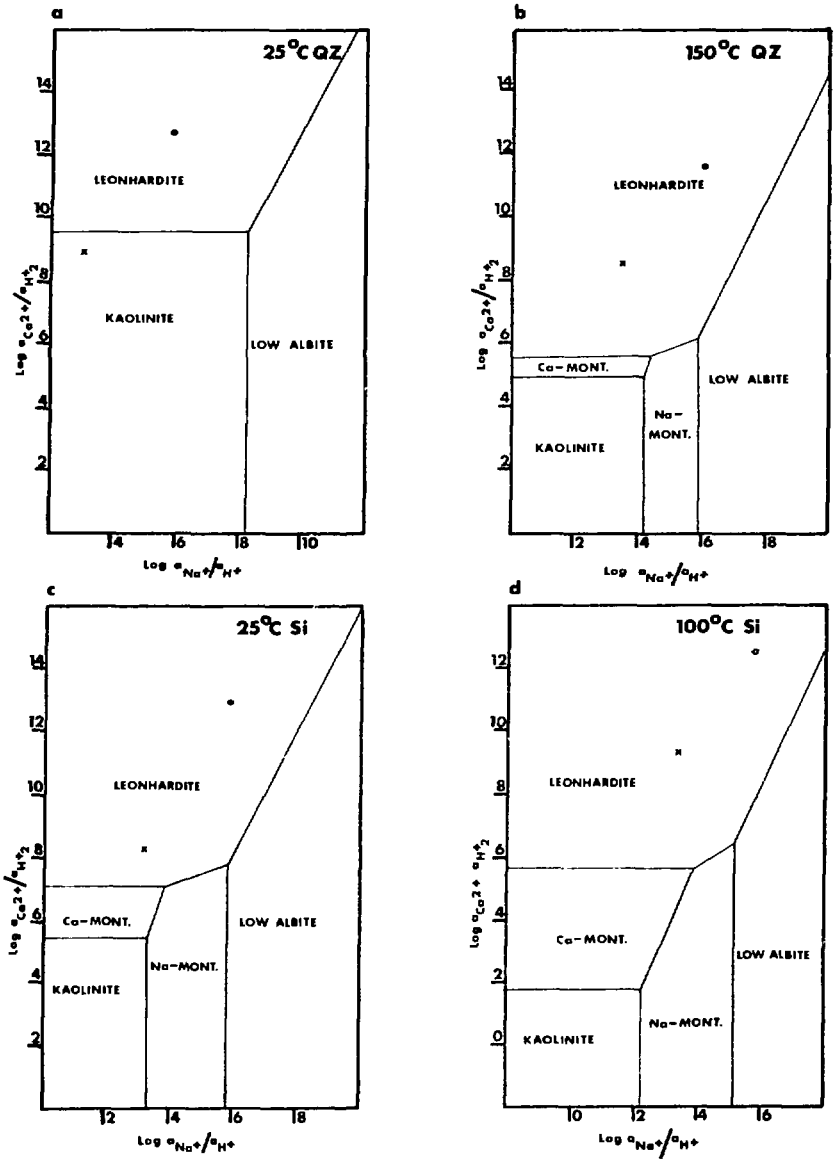

FIGURE 10: Theoretical Stability Fields in the System SiO_2-Al_2O_3-CaO-Na_2O-HCl (after Helgerson et al. [61])

QZ = Quartz Saturation; Si = Amorphous Silica Saturation
o = Standard Canadian Shield Saline Solution (SCSSS);
x = Granite Groundwater (GGW)

ISSN 0067-0367

To identify individual documents in the series we have assigned an AECL- number to each.

Please refer to the AECL- number when requesting additional copies of this document from

Scientific Document Distribution Office
Atomic Energy of Canada Limited
Chalk River, Ontario, Canada
KOJ 1JO

Price: $4.00 per copy

ISSN 0067-0367

Pour identifier les rapports individuels faisant partie de cette série nous avons assigné un numéro AECL- à chacun.

Veuillez faire mention du numéro AECL- si vous demandez d'autres exemplaires de ce rapport au

Service de Distribution des Documents Officiels
L'Energie Atomique du Canada Limitée
Chalk River, Ontario, Canada
KOJ 1JO

prix: $4.00 par exemplaire